MATEMATIKA, MJIM, Volume 38, Number 1, 1–20

Herschel-Bulkley Model for Mathematical Analysis of Blood Flow through an Asymmetric Stenosed Artery with Unsteady Reactive Solute Dispersion

Siti Nurul Aifa Mohd Zainul Abidin, Nurul Aini Jaafar* and Zuhaila Ismail

Department of Mathematical Sciences, Faculty of Science
Universiti Teknologi Malaysia, 81310 Skudai, Johor, Malaysia

*Corresponding author: nurulaini.jaafar@utm.my

Article history
Received: 6 December 2021
Received in revised form: 14 March 2022
Accepted: 21 March 2022
Published on line: 30 April 2022

Abstract This study examines the effects of chemical reaction, stenosis shape parameter and non-Newtonian behaviour on solute dispersion in blood flow via an asymmetric stenosed artery using the generalised dispersion model (GDM). The Herschel–Bulkley (H-B) fluid model, which consists of a yield stress and power-law index, is used to represent the non-Newtonian characteristics of blood in a narrow artery at a low shear rate. The impact of stenosis shape parameter, chemical reaction, power-law index and plug flow radius on the dispersion coefficient and effective axial diffusion of solute is shown. The findings showe that the aforementioned parameters significantly impact the overall process of the chemically reactive solute in a bulk flow. The dispersion coefficient and effective axial diffusion decrease with an increase in the chemical reaction rate, stenosis shape parameter and power-law index. As time passes, the dispersion process slows and becomes almost constant implying a steady state of diffusion. In short, this study provides further insights into the physiological processes involving in the dispersion of drugs and nutrients in the circulatory system.

Keywords Blood flow; Chemical reaction; Dispersion; Asymmetric stenosis; Herschel-Bulkley fluid.

Mathematics Subject Classification 65L05, 65L10, 76A05, 76R50, 76Z05.

1 Introduction

The investigation of solute dispersion in fluid flow is a vital concern due to the wide range of applications in various fields, such as chemical engineering, biomedical engineering, physiological fluid dynamics, environmental sciences, medical sciences and pharmacology. Taylor [1] was the first scientist to provide a theoretical and experimental background of the solute dispersion theory by omitting the axial diffusion term in the study. The dispersion theory was enhanced by Aris [2], where the author included the effect of axial molecular diffusion - known as Taylor-Aris dispersion theory. The latter theory was valid only for a prolonged

duration. In order to obtain an exact solution of the unsteady convective diffusion equation that is applicable at all times, Gill and Sankarasubramanian [3] proposed an alternative approach known as the generalised dispersion model (GDM). Several researchers, including Rana and Murthy [4]; Jaafar *et al.* [5] and Sankar *et al.* [6] have investigated the solute dispersion process using the approach proposed by Gill and Sankarasubramanian [3].

The present problem is based on the solute dispersion that undergoes a homogeneous reaction in the bulk flow which has significant applications in air pollution, gas absorption in an agitated tank, ester hydrolysis, catalysis, biochemical techniques, ceramic production, fibrous insulation, and crop-damaging through freezing [7]. The diffusion process becomes more complicated when the fluid is chemically reactive [8]. The chemical reaction can be classified either as a homogeneous or a heterogeneous reaction. The influence of chemical reactions in flowing fluid was assessed by Roy *et al.* [9], where the authors analysed the dependency of bulk flow reaction parameter on the flow velocities and dispersion coefficients of solute. In another study by Rana and Murthy [10], the effects of heterogeneous irreversible wall reactions on the dispersion of a chemical species in the pulsatile flow of blood were evaluated. Similarly, Roy *et al.* [11-12] conducted two successive studies that examined solute dispersion process in Newtonian and non-Newtonian fluids that was affected by the bulk flow reaction. Recently, Das *et al.* [13] investigated the effects of homogeneous and heterogeneous reactions on solute dispersion while considering the transverse and longitudinal directions.

Damaged and blocked arteries is a life-threatening disorders affecting a large percentage of human population worldwide [14] leading to cardiovascular anomalies and heart-related diseases, such as cardiac ischaemia, brain ischaemia, and cardiac arrest [15]. The progressive accumulation of low-density lipoproteins, cholesterol, cellular waste products, and other substances along the arterial wall causes a reduction of the arterial diameter and disturbs the normal blood flow [16]. The arterial wall gets thickened and hardened due to these accumulations. Consequently, a plaque is developed which ends up narrowing the artery, a condition known as atherosclerosis or stenosis. This study was designed to mitigate these heart-related disorders by improving the current body of knowledge regarding the underlying mechanisms and root causes. These findings might support the development of suitable bioengineering methods for their elimination. Overall, there is a substantial difference in blood flow between stenosed and normal arteries [17]. Abbas *et al.* [18] stated that the flow characteristics of blood are significantly affected due to the presence of stenosis. According to Shah [19] and Mishra and Siddiqui [20], it is challenging to resolve the solute dispersion issue when the blood flowing through an artery has stenosis in certain regions. Sriyab [21] and Sankar *et al.* [22] stated that the analysis of blood flow in stenotic arteries is vital in understanding circulatory disorders. According to Hossain and Haque [23] and Freidoonimehr *et al.* [24], the shape and degree of stenosis of a stenotic coronary artery have significant impacts on arterial blockage. Prashantha and Anish [25] emphasized the importance of understanding haemodynamics in the post-stenotic of asymmetric stenosis. The authors highlighted that about 70 to 80% of cardiovascular diseases occur in complex geometries. Given this, the majority of recently published studies concentrated on issues related to blood flow in arteries with complex geometries in the absence of chemically reactive solute [26-28]. It is of utmost importance to concurrently study the solute dispersion in the presence of chemically active solute at the bulk of the flow having stenosis in the arterial wall in order to analyse the rheological behaviour of blood flow in a diseased state.

Recently, several researchers' interests have been drawn towards the topic of solute dispersion either in a steady or unsteady flow of non-Newtonian fluids in a tube/channel. This is due to its widespread applications in biochemical processing, cardiovascular flows, and polymers. Notably, using the method of GDM, the solute dispersion issues for non-Newtonian fluids were resolved by several researchers. This method consolidates a set of solutions that describe the entire dispersion process at all times. Using the GDM, Tiwari *et al.* [29] analysed the unsteady solute dispersion in two-fluid flowing through narrow tubes. Rana and Liao [30] investigated the axial dispersion of a solute in a pulsatile flow of Herschel-Bulkley (H-B) fluid through a straight circular tube with wall absorption using GDM. Likewise, Ratchagar and Vijayakumar [31] employed the GDM to evaluate the dispersion of a solute in blood flow with the inclusion of chemical reaction and magnetic field using a non-Newtonian fluid model. They discovered that the dispersion coefficient which describes the entire diffusion process decreases due to chemical reaction and shows a reciprocal behaviour in the absence of chemical reaction. Rana and Murthy [32] conducted a comparative study of solute dispersion among single and two-phase fluid models using GDM. Other researchers applied GDM to study the dispersion of a solute in non-Newtonian fluid flow [33-35].

Blood has been described to behave like a H-B fluid by several authors [36-37]. The yield stress, apparent viscosity, and the power-law index are the main three rheological parameters that characterise or influence the H-B fluid. This fluid model is advantageous because with suitable choice of the parameters could reduce the constitutive equation of H-B fluid to the power-law, Newtonian, and Bingham fluid models [38]. H-B fluids include shear thickening and shear thinning properties that are used in describing rheological properties of drilling fluids, greases, starch pastes, colloidal suspensions, paints, toothpaste, lubricant in roller-bearing and biological fluids like blood [39-40]. Furthermore, biomedicine, petroleum industries, polymer industries, and blood oxygenators developers are some of the several applications of H-B fluid [41]. Despite the velocity profiles of blood flow are not compatible with the Casson fluid in arterioles having diameters less than 65 H-B fluid is capable of explaining the same condition. Presently, most researchers are adopting the H-B fluid model for issues relating to non-Newtonian fluid [42-44].

Hence, based on previous works in the literature, there is a lack of studies on the problem of solute dispersion in blood flow with the inclusion of a chemically reactive species in an asymmetry stenosed artery using GDM. The study of solute dispersion in a non-Newtonian fluid is vital to produce realistic results that represent physical problems better. Furthermore, the knowledge of the rheological parameters is necessary to understand the effects of non-Newtonian rheology on solute dispersion. By solving this problem, the transport coefficients of solute in narrow arteries at a low shear rate can be predicted. Specifically, the contributions of the paper are twofold, firstly to evaluate the effects of reactive species in an asymmetry stenosed artery using GDM that was only addressed individually in previous studies, and secondly to analyse the rheological behaviour of non-Newtonian fluid in a stenosed artery.

2 Mathematical Formulation

Suppose a reactive chemical solute is moving through a miscible fluid-containing tube and undergoing a first-order reaction in the bulk flow. The blood flow is assumed to be steady, laminar, axially symmetrical, incompressible and fully developed unidirectionally.

2.1 Governing Equations

The cylindrical polar coordinates $(\overline{r}, \overline{\psi}, \overline{z})$ where $\overline{r}$ and $\overline{z}$ denote the radial and axial coordinates, respectively and $\overline{\psi}$ is the azimuthal angle is considered. This work excludes fluid velocity in the $\overline{r}$ direction since its magnitude is negligibly small and only accounts for the fluid velocity in the $\overline{z}$ direction. Therefore, $\overline{u}_{\overline{r}} = \overline{u}_{\overline{\psi}} = 0$ [45]. The simplified forms of momentum equations in the axial and radial directions, respectively:

$$\frac{\partial \bar{p}}{\partial \bar{z}} = -\frac{1}{\bar{r}}\frac{\partial}{\partial \bar{r}}(\bar{r}\bar{\tau}), \tag{1}$$

$$\frac{\partial \bar{p}}{\partial \bar{r}} = 0, \tag{2}$$

where $\partial\overline{p}/\partial\overline{z}$ is the pressure gradient in the axial direction and $\overline{\tau}$ is the shear stress. The unsteady convective–diffusion equation [46] with first-order chemical reaction that govern the mass transport is written as follows:

$$\frac{\partial \bar{C}}{\partial \bar{t}} = -\bar{u}\frac{\partial \bar{C}}{\partial \bar{z}} + D_m\left(\frac{1}{\bar{r}}\frac{\partial}{\partial \bar{r}}\left(\bar{r}\frac{\partial \bar{C}}{\partial \bar{r}}\right) + \frac{\partial^2 \bar{C}}{\partial \bar{z}^2}\right) - \bar{\beta}\bar{C}, \tag{3}$$

where $\overline{C}$ denotes the solute concentration per unit volume, $\overline{t}$ is the time variable, D_m denotes the coefficient of mass diffusion and $\overline{\beta}$ denotes the parameter of the chemical reaction.

2.2 Initial and Boundary Conditions

The non-linear system of a differential equation for the unknown shear stress $\overline{\tau}$ defined by equation (1) is based on the following boundary condition:

$$\bar{\tau} \text{ is finite at } \bar{r} = 0. \tag{4}$$

The fluid is regarded as vicious since it adheres to the arterial wall, hence the no-slip boundary condition is given by

$$\bar{u} = 0 \text{ at } \bar{r} = \bar{R}\left(\bar{z}\right). \tag{5}$$

Following [3], the initial and boundary conditions are as follows:

$$\bar{C}\left(\bar{r}, \infty, \bar{t}\right) = 0, \tag{6}$$

$$\frac{\partial \bar{C}}{\partial \bar{r}}\left(0, \bar{z}, \bar{t}\right) = 0 = \frac{\partial \bar{C}}{\partial \bar{r}}\left(\bar{R}(\bar{z}), \bar{z}, \bar{t}\right). \tag{7}$$

2.3 Geometry of Stenosis

According to Sankar and Lee [47], the geometry of the asymmetric stenosis in the dimensional form is denoted as follows:

$$\bar{R}(\bar{z}) = \begin{cases} 1 - \bar{A}\left[\bar{l}_0{}^{m-1}(\bar{z} - \bar{d}) - (\bar{z} - \bar{d})^m\right], & \bar{d} \le \bar{z} \le \bar{d} + \bar{l}_0, \\ 1, & \text{otherwise}, \end{cases} \tag{8}$$

where $\overline{A}=\left(\overline{\delta}/R_0\overline{l}_0\right)m^{(m/m-1)}$, R_0 is the arterial radius, $\overline{\delta}$ is the height of stenosis, $\overline{l}_0$ is the length of the stenosis, $\overline{z}$ is the longitudinal (axial) distance, $\overline{r}$ is the transverse (radial) distance, $\overline{d}$ is

the stenosis location, $\overline{L}$ is the artery length, m is the stenosis shape parameter and $\overline{R}(\overline{z})$ is the stenotic artery radius. Figure 1 illustrates the geometry of an asymmetric stenosed artery under consideration. The arterial segment is assumed to be long enough that the entrance, endpoint and distinctive wall effects can be disregarded. The stenosed artery is assume to be rigid since the stenosis is lodged in the lumen. According to Mishra and Siddiqui [20], symmetric stenosis has a stenosis shape parameter value of 2, whereas asymmetric stenosis has a stenosis parameter value of 3–6.

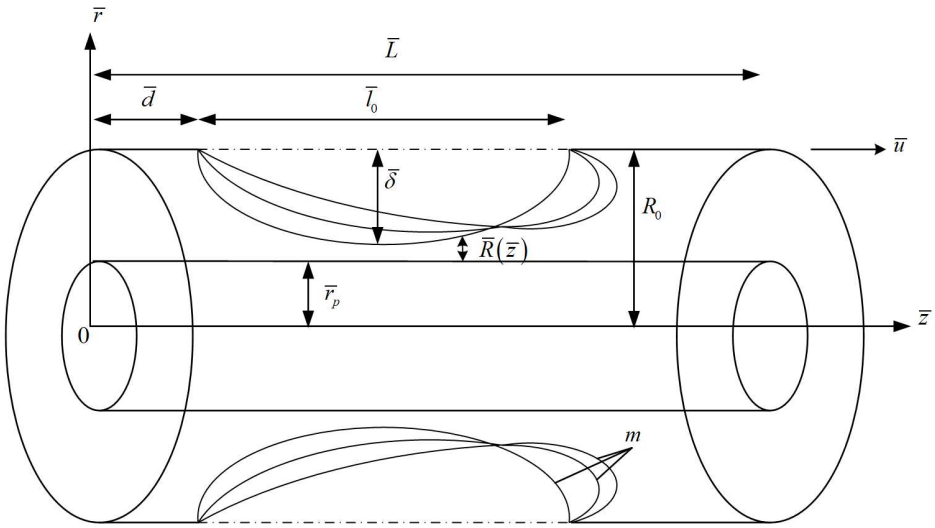

Figure 1: The geometry of the asymmetric stenosed artery

2.4 Non-dimensionalisation

The following are the non-dimensional variables:

$$\begin{aligned} &C = \frac{\bar{C}}{\bar{C}_0}, u = \frac{\bar{u}}{u_0}, u_m = \frac{\bar{u}_m}{u_0}, r = \frac{\bar{r}}{R_0}, r_p = \frac{\bar{r}_p}{R_0}, t = \frac{D_m \bar{t}}{R_0^2}, z = \frac{D_m \bar{z}}{R_0^2 u_0}, \tau = \frac{\bar{\tau}}{(\eta_H u_0/R_0)^{\frac{1}{n}}}, \\ &\tau_y = \frac{\bar{\tau}_y}{(\eta_H u_0/R_0)^{\frac{1}{n}}}, \delta = \frac{\bar{\delta}}{R_0}, l_0 = \frac{\bar{l}_0}{R_0}, R(z) = \frac{\bar{R}(\bar{z})}{R_0}, \beta = \sqrt{\frac{R_0^2 \bar{\beta}}{D_m}}, \end{aligned} \tag{9}$$

where C is the solute concentration, u is the velocity, u_m is the average velocity, u_0 is the fluid characteristics velocity (centreline velocity), r is the radial distance, r_p is the radius of the plug core field, z is the longitudinal distance, t is the time, τ_y is the yield stress and β is the rate of chemical reaction. The transport equation and the geometry of the asymmetric stenosis in the non-dimensional form are

$$\frac{\partial C}{\partial t} + u\frac{\partial C}{\partial z} = \left(\frac{1}{r}\frac{\partial}{\partial r}\left(r\frac{\partial C}{\partial r}\right) + \frac{1}{Pe^2}\frac{\partial^2 C}{\partial z^2}\right) - \beta^2 C, \tag{10}$$

where $Pe = R\,(z)\ \ u_0/D_m$.

$$R(z) = \begin{cases} 1 - A\left[{l_0}^{m-1}(z-d) - (z-d)^m\right], & d \le z \le d + l_0, \\ 1, & \text{otherwise}, \end{cases} \tag{11}$$

where $A{=}(\delta/R_0 l_0)\, m^{(m/m-1)}$. Singh *et al.* [48] defined the H-B fluid constitutive equation as follows:

$$\frac{du}{dr} = \begin{cases} -(\tau-\tau_y)^n\,, & \text{if } \tau \geq \tau_y \text{ and } r_p \leq r \leq R(z)\,, \\ 0\,, & \text{if } \tau < \tau_y \text{ and } 0 \leq r < r_p, \end{cases} \tag{12}$$

where n is the power-law index. Equation (12) implies that normal shear flow occurs in the field when $\tau \geq \tau_y$, while the plug flow field occurs when $\tau < \tau_y$. Dash et al. [34] asserted that whenever the yield stress exceeds the shear stress, the fluid in the region does not flow but is instead carried along at a constant velocity by the fluid particles in the adjoining shear flow region.

2.5 Method of Solution

The non-dimensional velocity of blood flow in the non-plug flow field is defined as $u_+(r)$ and written as follows to distinguish it from the velocity in the plug flow field:

$$u_+(r) = 1 - \tfrac{r^{n+1}}{R^{n+1}(z)} - (n+1)\,\tfrac{r_p}{R(z)}\left(1 - \tfrac{r^n}{R^n(z)}\right) + \tfrac{n(n+1)}{2}\tfrac{r_p^2}{R^2(z)}\left(1 - \tfrac{r^{n-1}}{R^{n-1}(z)}\right), \quad \text{if } \tau \geq \tau_y \text{ and } r_p \leq r \leq R(z)\,, \tag{13}$$

where r_p is the yield stress over a pressure gradient that can be described as the plug core radius. By evaluating equation (13) at $r = r_p$, the non-dimensional plug flow field velocity can be written as:

$$u_-(r_p) = 1 - (n+1)\,\frac{r_p}{R(z)} + \frac{n(n+1)}{2}\frac{r_p^2}{R^2(z)} - \frac{n(n-1)}{2}\frac{{r_p}^{n+1}}{R^{n+1}(z)}, \text{if } \tau < \tau_y \text{ and } 0 \leq r < r_p\,. \tag{14}$$

The mean velocity in non-dimensional is interpreted as:

$$u_m = \tfrac{(n+1)}{(n+3)}\left(1 - \tfrac{n(n+3)}{(n+2)}\tfrac{r_p}{R(z)} - \tfrac{n(n+3)}{(n+2)}\tfrac{r_p}{R(z)} + \tfrac{n(n-1)(n+3)}{2(n+1)}\tfrac{{r_p}^2}{R(z)^2} - \tfrac{\left(n^4+2n^3-5n^2-6n+4\right)}{2(n+1)(n+2)}\tfrac{r_p^{n+3}}{R^{n+3}(z)}\right)\,. \tag{15}$$

The solute convection over a plane moving at an average velocity u_m is considered in such a way that the axis moves with the average speed of the fluid. A new coordinate system (r, z_1, t) that includes an axial coordinate z_1 is introduced, where z_1 is expressed as follows

$$z_1 = z - u_m\, t. \tag{16}$$

Following the approach by Gill *et al.* [3] who employed GDM, the solution from equation (10) is assumed to be a derivative series expansion involving $\partial C_m/\partial z_1^i$ as follows:

$$C(r, z_1, t) = C_m(z_1, t) + \sum_{i=R(z)}^{\infty} f_i(r,t)\,\frac{\partial^i C_m(z_1,t)}{\partial z_1^i}, \tag{17}$$

where

$$C_m(z_1,t) = 2\int_0^{R(z)} C(r, z_1, t)\; r\; dr \tag{18}$$

is the average solute concentration across the fragmentary area. The partial differential equation of the average solute concentration with the chemical reaction is obtained by substituting equation (17) into equation (10) as follows:

$$\begin{aligned}\frac{\partial C_m}{\partial t}+(u-u_m)\frac{\partial C_m}{\partial z_1^1}-\frac{1}{Pe^2}\frac{\partial^2 C_m}{\partial z_1^2}+\sum_{i=1}^{\infty}\Big(\Big(\frac{\partial f_i}{\partial t}-l^2 f_i\Big)\frac{\partial^i C_m}{\partial z_1^i}+(u-u_m)f_i\frac{\partial^{i+1}C_m}{\partial z_1^{i+1}}\\ -\frac{1}{Pe^2}f_i\frac{\partial^{i+2}C_m}{\partial z_1^{i+2}}+f_i\frac{\partial^{i+1}C_m}{\partial z_1^{i+1}\partial t}+\beta^2 f_i\frac{\partial^i C_m}{\partial z_1^i}\Big)+\beta^2 C_m=0,\end{aligned} \tag{19}$$

where $l^2=1/r\partial/\partial r\,(r\partial/\partial r)$. Dash *et al.* [34] stated that the process of distributing $C_m(z,t)$ is diffusive from the beginning of time, hence using GDM with the inclusion of chemical reaction as suitable functions of time t yields the following:

$$\frac{\partial C_m}{\partial t}=\sum_{i=1}^{\infty}K_i(t)\frac{\partial^i C_m}{\partial z_1^i}(z_1,t)-\beta^2 C_m(z_1,t), \tag{20}$$

where $K_1(t)$ is the longitudinal convection coefficient and $K_2(t)$ is the longitudinal diffusion coefficient. Since $K_2(t)$ depicts the entire dispersion process with regards to simple diffusion process in the axial direction z_1, the parameter is also known as the dispersion coefficient. Substituting equation (20) into equation (19) and grouping the coefficients $\partial^i C_m/\partial z_1^i$ for $i=1,\ 2,\dots$ yields:

$$\begin{aligned}\Big[K_1(t)+(u-u_m)+\frac{\partial f_1}{\partial t}-l^2 f_1+\beta^2 f_1\Big]\frac{\partial C_m}{\partial z_1^1}+\Big[-\frac{1}{Pe^2}+(u-u_m)f_1+f_1K_1(t)+K_2(t)\\ +\frac{\partial f_2}{\partial t}-l^2 f_2+\beta^2 f_2\Big]\frac{\partial^2 C_m}{\partial z_1^2}+\sum_{i=1}^{\infty}\Big[-\frac{1}{Pe^2}f_i+(u-u_m)f_{i+1}+K_{i+2}(t)+\frac{\partial f_{i+2}}{\partial t}-l^2 f_{i+2}\\ +\beta^2 f_{i+2}+\sum_{j=1}^{i+1}K_j(t)f_{i+2-j}\Big]\frac{\partial^{i+2}C_m}{\partial z_1^{i+2}}=0.\end{aligned} \tag{21}$$

The infinite system of partial differential equations is derived by equating $\partial^i C_m/\partial z_1^i$ coefficients to zero for $i=1,\ 2,\dots$ as follows:

$$\frac{\partial f_1}{\partial t}-l^2 f_1+u-u_m+K_1(t)+\beta^2 f_1=0, \tag{22}$$

$$\frac{\partial f_2}{\partial t}-l^2 f_2+[u-u_m+K_1(t)]f_1+K_2(t)-\frac{1}{Pe^2}+\beta^2 f_2=0, \tag{23}$$

$$\frac{\partial f_{i+2}}{\partial t}-l^2 f_{i+2}+[u-u_m+K_1(t)]f_{i+1}+\left[K_2(t)-\frac{1}{Pe^2}\right]f_i+\beta^2 f_{i+2}+\sum_{j=3}^{i+2}K_j(t)f_{i+2-j}=0, \tag{24}$$

with $f_0=1$. The initial and boundary conditions for f_i are

$$f_i(r,0)=0, \tag{25}$$

$$\frac{\partial f_i}{\partial r}(0,t)=0=\frac{\partial f_i}{\partial r}(R(z),t). \tag{26}$$

Using equations (17) and (18), the solvability condition is obtained as follows:

$$\int_0^{R(z)} f_i\ r\ dr=0. \tag{27}$$

The longitudinal convection coefficient $K_1(t)$ is calculated by multiplying equation (22) by r and subsequently integrating the result from zero to one with respect to r. After using of equation (27), the formula for $K_1(t)$ is given as:

$$K_1(t) = -2\int_0^{R(z)} (u - u_m)\ r\ dr. \tag{28}$$

The same approach is applied in equations (23) and (24), which yield the following transport coefficients:

$$K_2(t) = \frac{1}{Pe^2} - 2\int_0^{R(z)} f_1\ u\ r\ dr, \tag{29}$$

$$K_{i+2}(t) = -2\int_0^{R(z)} f_{i+1}\ u\ r\ dr, \quad i = 1, 2, 3, ... \tag{30}$$

The solutions to the non-homogeneous parabolic differential equations for equations (22), (23) and (24) are divided into two parts as follows:

$$f_1(r,t) = f_{1s}(r) + f_{1t}(r,t), \tag{31}$$

where $f_{1s}(r)$ and $f_{1t}(r,t)$ are the dispersion functions in the steady-state and transient state, respectively. The dispersion function $f_{1t}(r,t)$ characterizes the time-dependent aspect of the solute dispersion. Substituting equation (31) into (22) yields:

$$\frac{\partial f_{1s}}{\partial t} + \frac{\partial f_{1t}}{\partial t} - l^2 f_{1s} - l^2 f_{1t} + (u - u_m) + \beta^2 f_{1s} + \beta^2 f_{1t} = 0. \tag{32}$$

Since $\partial f_{1s}/\partial t = 0$, there is no change in dispersion with time under a steady state. By rearranging the coefficients in equation (32), the following differential equations are obtained:

$$l^2 f_{1s} - (u - u_m) - \beta^2 f_{1s} = 0, \tag{33}$$

$$\frac{\partial f_{1t}}{\partial t} = l^2 f_{1t} - \beta^2 f_{1t}. \tag{34}$$

By substituting equation (31) into equations (25) and (26), then grouping $f_{1s}(r)$ and $f_{1t}(r,t)$, the initial conditions of $f_{1t}(r,t)$ and the boundary conditions of $f_{1s}(r)$ and $f_{1t}(r,t)$ are obtained as follows:

$$f_{1t}(r,0) = -f_{1s}(r), \tag{35}$$

$$\frac{df_{1s}}{dr}(r=0) = 0 = \frac{df_{1s}}{dr}(r = R(z)), \tag{36}$$

$$\frac{\partial f_{1t}}{\partial r}(0,t) = 0 = \frac{\partial f_{1t}}{\partial r}(R(z), t). \tag{37}$$

The solvability condition for $f_{1s}(r)$ and $f_{1t}(r,t)$ is given as:

$$\int_0^{R(z)} f_{1t}\ r\ dr = -\int_0^{R(z)} f_{1s}\ r\ dr. \tag{38}$$

The differential equation of dispersion function at steady state in a plug flow field is given as:

$$\frac{1}{r}\frac{d}{dr}\left(r\frac{df_{1s_-}}{dr}\right)-(u_- - u_m)-\beta^2 f_{1s_-}=0, \quad \text{if } 0\le r<r_p. \tag{39}$$

Based on equation (34), the outer flow field becomes:

$$\frac{1}{r}\frac{d}{dr}\left(r\frac{df_{1s_+}}{dr}\right)-(u_+ - u_m)-\beta^2 f_{1s_+}=0, \quad \text{if } r_p\le r\le R(z). \tag{40}$$

Using Wolfram Mathematica, equation (39) is solved numerically subject to the boundary condition (36), yielding the steady dispersion function in the plug flow field as follows:

$$f_{1s_-}(r)=-\tfrac{1}{\beta^2}\left(\tfrac{2}{(n+3)}+\tfrac{2(n+1)}{(n+2)}\tfrac{r_p}{R(z)}+n\tfrac{r_p^2}{R^2(z)}-\tfrac{n(n-1)}{2}r_p^{n+1}R^{-n-1}(z)+\tfrac{\left(n^4+2n^3-5n^2-6n+4\right)}{2(n+2)(n+3)}r_p^{n+3}R^{-n-3}(z)\right)+S_1J_0(i\beta r), \quad \text{if } 0\le r<r_p, \tag{41}$$

where J_0 is the Bessel function of the first kind of order zero and S_1 is a constant. In the outer flow field in the range of $r_p \le \mathrm{r} \le R(z)$, the steady dispersion function can be obtained numerically by solving equation (40) subject to the boundary condition (26). The expression S_1 is obtained using equation (27). Equation (34) is solved using the variable separation method and Bessel function, subject to the boundary conditions (35) and (37). The solution of $f_{1t}(r,t)$ is as follows:

$$f_{1t}(r,t)=e^{-\beta^2 t}\sum_{m=1}^{\infty}A_m\, e^{-\lambda_m^2 t}\, J_0(\lambda_m\, r), \tag{42}$$

where

$$A_m=-\frac{\int_0^{R(z)}J_0(\lambda_m\, r)\;\, f_{1s}(r)\, r\, dr}{\int_0^{R(z)}J_0^2(\lambda_m\, r)\;\, r\, dr}=-\frac{2}{J_0^2(\lambda_m)}\int_0^{R(z)}J_0(\lambda_m\, r)\;\, f_{1s}(r)\, r\, dr. \tag{43}$$

The eigenvalues λ_m are the roots of equation $J_1(r)=0$. J_0 and J_1 denote the Bessel functions of the first kind of order zero and one, respectively. The dispersion coefficient $K_2(t)$ is a measure of the effectiveness of solute dispersion in the blood flow. Dash *et al.* [34] and Ramana *et al.* [35] stated that the total reduction in solute dispersion caused by the fluid yield stress at a constant pressure gradient can be measured by subtracting equation (31) with $1/Pe^2$ and multiplying the result with 192, yielding the following:

$$192\left(K_2(t)-\frac{1}{Pe^2}\right)=-2\int_0^{R(z)}f_1\, u\, r\, dr. \tag{44}$$

The influence of a distorted velocity profile of H-B fluid on unsteady solute dispersion with a chemical reaction in a circular pipe is defined as follows:

$$\frac{\left(K_2(t)-\frac{1}{Pe^2}\right)}{\left(K_2^N(t)-\frac{1}{Pe^2}\right)}, \tag{45}$$

where $K_2^N(t)$ is the longitudinal diffusion coefficient (dispersion coefficient) for the Newtonian fluid. Once $K_2(t)$ is determined, $f_2(r,t)$ can be obtained from equation (23) using a similar method used to obtain $f_1(r,t)$. Substituting $f_2(r,t)$ into equation (24) when $i = 1$ yields $K_2(t)$ and similarly for $i = 2, 3, \ldots$, one can find $f_3(r,t)$, $K_4(t)$, $f_4(r,t)$, $K_5(t)$ and so on from equations (24) and (30). Since the coefficient $K_3(t)$ is negligible and the solutions obtained for $f_1(r,t)$ and $K_3(t)$ are lengthy and cumbersome, the computation of $K_{i+2}(t)$ and $f_{i+1}(r,t)$ for $= 1, 2, \ldots$ are disregarded. Equation (45) measures the total reduction in solute dispersion of H-B fluid relative to Newtonian fluid due to the presence of chemically reactive solute at the bulk of the flow.

3 Results and Discussion

This study aims to examine the behaviour of blood flow for unsteady dispersion in a narrow circular pipe to simulate the involvement of asymmetry stenosis and reactive species in the bulk flow. The study is also intended to depict non-Newtonian behaviour and the impacts of various physical parameters on the the dispersion coefficient and effective axial diffusion of the solute. The parameter values used in this study are in the following range: yield stress r_p : 0–0.2 [49], power-law index n : 0.75–2.0 [49], rate of chemical reaction β : 0.1–2.5 [50-51], stenosis height δ : 0.01 [40], amplitude A : 0.1–0.5 [52] and stenosis shape parameter m : 2.0–3.8 [52].

3.1 Validation of Results

Figure 2 illustrates the validation results of the steady dispersion function f_{1s}, unsteady dispersion function f_{1t} and dispersion function f_1 for the presence and previous study in the absence of stenosis with $n = 0.95$, $\beta = 0.1$, $R(z) = 1$ and $r_p = 0.1$. The aforementioned figures are found to be in good agreement with Sankar et al. [6] and Jaafar [53]. For validation purposes, the geometry of the stenosed artery $R(z)$ is set to one.

3.2 Dispersion Coefficient

Figure 3 (a) depicts the variation of dispersion coefficient over time t for various chemical reaction rate parameter β when $t = 0.1$, $n = 0.95$, $r_p = 0.1$, $\delta = 0.01$, $R(z) = 0.827, l_0 = 3, d = 2$, $z = 4$ and $m = 3$. The dispersion coefficient decreases as the chemical reaction parameter increases, indicating that the solute diffuses more slowly in the longitudinal direction as the chemical reaction rate increases. There is a slight difference in the dispersion coefficient when $\beta = 0.1$ and 1 before the dispersion coefficient reaches its steady-state. The results imply that as the chemical reaction rate increases, the solute diffuses slightly into the blood protein and acquires a steady longitudinal diffusion as time increases to $t = 0.4$. These findings also suggest that because the degree of solute binding to blood proteins increases, the chemical reaction tends to reduce solute dispersion. The solute longitudinal diffusion coefficient is similar until $t = 0.02$, at which point it increases monotonically as the chemical reaction rate increases.

Figure 3 (b) shows the variation of the dispersion coefficient over time t for various stenosis shape parameter m when $\beta = 0.1$, $t = 0.1$, $n = 0.95, \delta = 0.01, r_p = 0.1, l_0 = 3, d = 2$ and $z = 4$. The stenosis takes on a symmetric shape when the stenosis shape parameter $m = 2$. The dispersion coefficient eventually has a common time of $t = 0.02$. As the stenosis

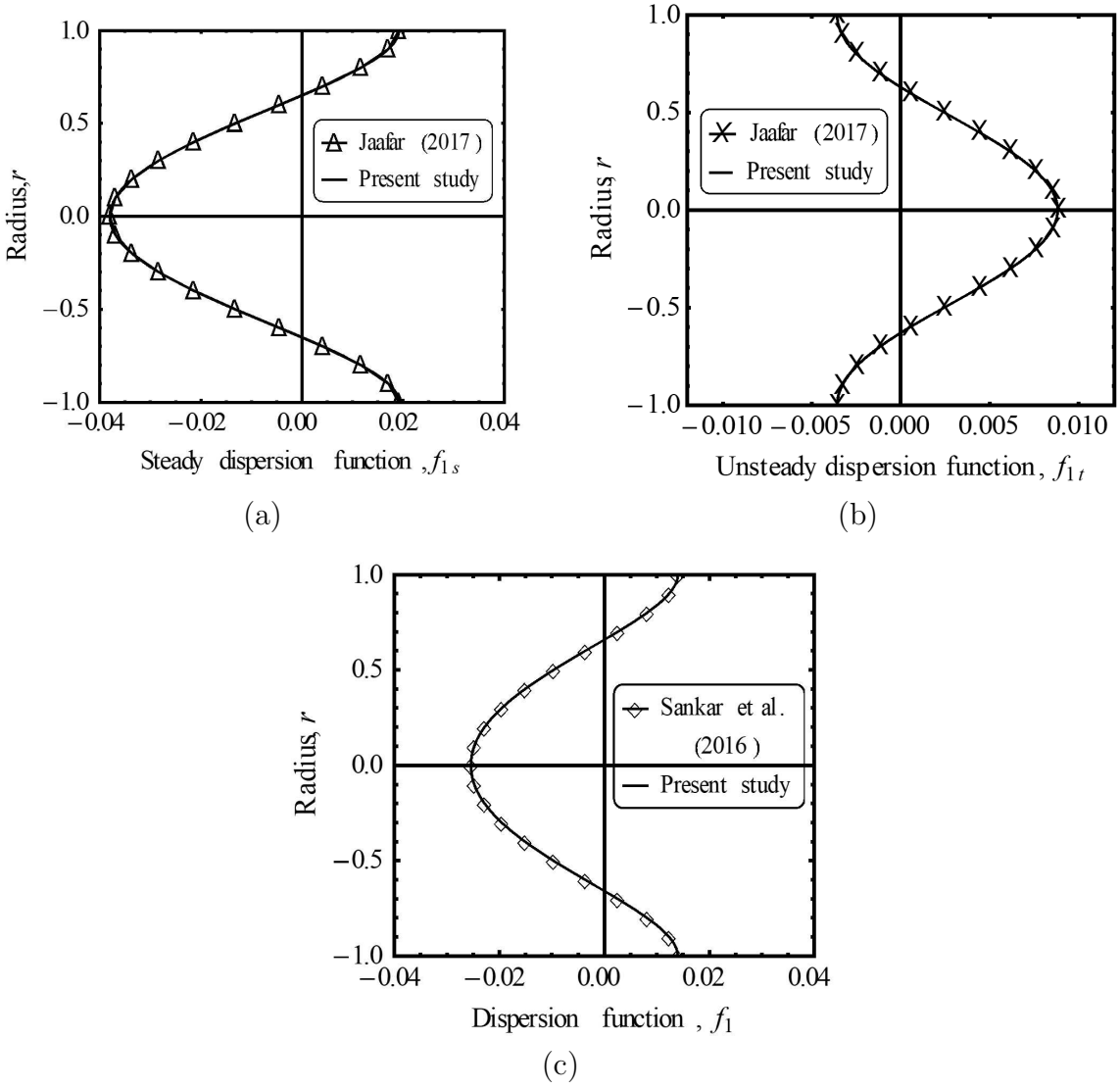

Figure 2: The parameters are fixed at $n = 0.95,\ \beta = 0.1,\ R(z) = 1,\ \delta = 0$ and $r_p = 0.1$ (a) steady dispersion function f_{1s}, (b) unsteady dispersion function f_{1t} with $t = 0.1$ and (c) dispersion function f_1 with $t = 0.1$

shape parameter increases from $m = 2.0,\ 2.5,\ 3.0,\ 3.5$ to 3.8, the dispersion coefficient also increases until $t = 0.02$, after which it decreases significantly until it almost becomes constant at $t = 0.3$. This is because initially the solute dispersion by convection takes place more rapidly than the molecular diffusion. Thus, the asymptotic value of the dispersion coefficient is attained immediately after the injection of the solute. The stenosis shape parameter m controls the shape of stenosis and affects the velocity profile. The radius of the stenosed artery decreases from $R(z) = 0.997,\ 0.993,\ 0.983,\ 0.962$ to 0.940 with the increase of the stenosis shape parameter. These results imply that the stenosis shape parameter affects the radius of the stenosed artery as the solute diffuses in the blood.

Figure 4 (a) illustrates the variation of the dispersion coefficient over time t for various plug core radius r_p when $\beta = 0.1,\ t = 0.1,\ n = 0.95,\ R(z) = 0.827,\ \delta = 0.01,\ l_0 = 3,\ d = 2,\ z = 4$

and $m = 3$. The dispersion coefficient K_2 depends on the non-Newtonian rheological parameter, which is the fluid yield stress, through its dependence on the plug flow parameter r_p. The dispersion coefficient is shown to decrease significantly as the plug core radius increases. The dispersion coefficient rises rapidly from $t = 0$ to 0.1, then slowly from $t = 0.1$ to 0.26, and becomes almost constant from $t = 0.26$ to 0.5. This figure exhibits two distinctive behaviours as mentioned in equation (29). The non-linear behaviour of the plot for the unsteady state of diffusion is shown by the non-uniform solute concentration in the blood flow, whereas the linear behaviour of the plot for the steady state of diffusion is shown by the uniform or saturated solute concentration. These findings imply that the solute diffuses vigorously in the blood (represented by the H-B fluid) at the start of the dispersion process, then slowly until it becomes almost constant as time passes. The yield stress is related to the non-Newtonian nature of the fluid, with the increase in yield stress increasing blood viscosity. The yield stress is also associated with the radius of the plug region through the expression $\tau_y = r_p/2$, indicating that the radius of the plug region increases with the increase of yield stress.

Figure 4 (b) indicates the variation of dispersion coefficient over time t for various fluids for $\beta = 0.1,\ t = 0.1,\ R(z) = 0.827,\ \delta = 0.01,\ l_0 = 3,\ d = 2,\ z = 4\text{and}m = 3$. The dispersion coefficient decreases when the power-law index n and yield stress increase. The dispersion coefficient is higher when $n = 0.95$ (H-B fluid) than when $n = 1$ (Bingham fluid). The dispersion coefficient is lower when $r_p = 0.2$ (H-B fluid) than when $r_p = 0$ (power-law fluid). The viscosity of the fluid increases as the power-law index and yield stress increase, hence blood travels faster along the axial distance. The dispersion coefficient of the Newtonian fluid model is found to be marginally higher than that of the H-B fluid and Bingham fluid models and only slightly higher than the power-law fluid model. The solute dispersion coefficient for the Newtonian fluid model obtained in this study conforms with the results obtained by Gill et al. [3].

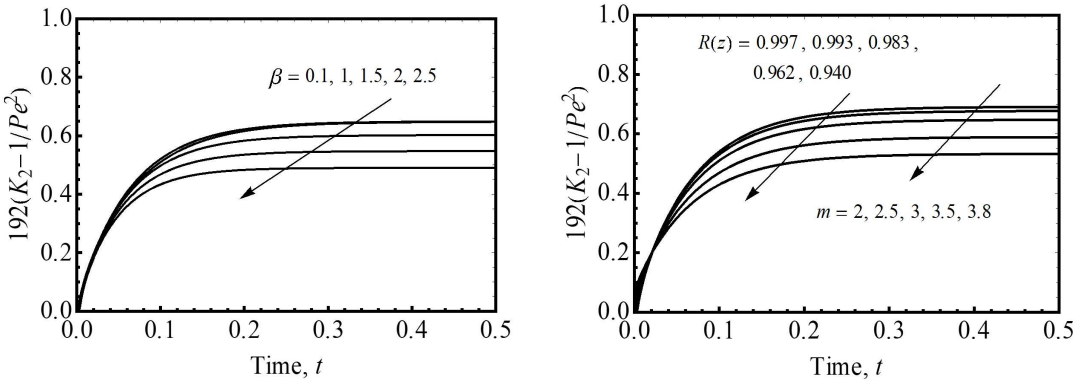

Figure 3: Variation of dispersion coefficient over time t when $t = 0.1,\ n = 0.95,\ \delta = 0.01,\ l_0 = 3,\ d = 2$ and $z = 4$ for (a) various chemical reaction rate parameter β (b) various stenosis shape parameter m

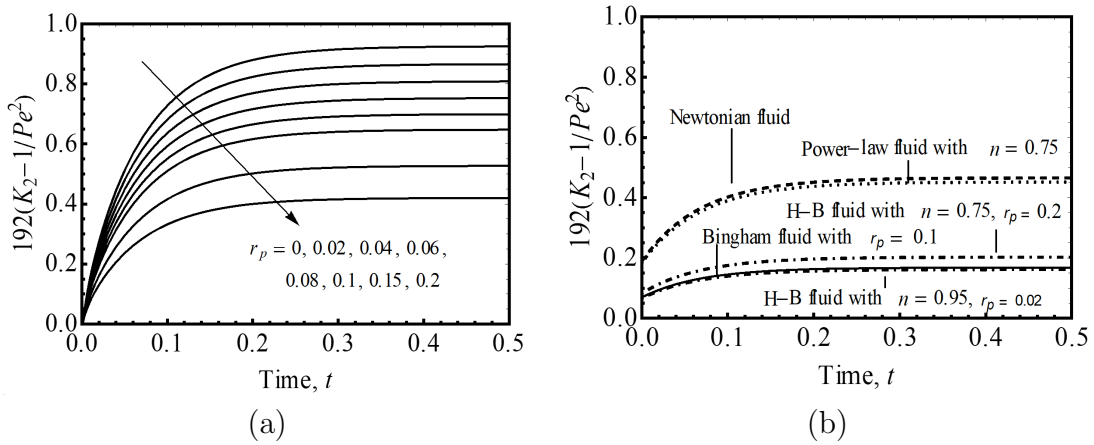

Figure 4: Variation of dispersion coefficient over time t when $\beta = 0.1,\ t = 0.1,\ R(z) = 0.827,\ \delta = 0.01,\ l_0 = 3,\ d = 2, z = 4$ and $m = 3$ for (a) various plug core radius r_p (b) various fluids

3.3 Effective Axial Diffusion

Figure 5 (a) depicts the variation of effective axial diffusion over time t for various chemical reaction rate parameter β when $t = 0.1,\ n = 0.95,\ r_p = 0.1,\ \delta = 0.01,\ R(z) = 0.827,\ l_0 = 3,\ d = 2,\ z = 4$ and $m = 3$. The effective axial diffusion increases as the chemical reaction rate increases from the beginning until $t = 0.23$, after which it remains constant. This implies that the solute diffuses vigorously in the blood proteins as the chemical reaction progresses. As the amount of solute that undergoes a chemical reaction in the bulk flow increases from $\beta = 0.1,\ 1.0,\ 1.5,\ 2.0$ to 2.5, more solutes react with the fluid, increasing the solute dispersion until it reached a steady-state of diffusion.

Figure 5 (b) describes the variation of effective axial diffusion over time t for various stenosis shape parameter m when $\beta = 0.1,\ t = 0.1,\ n = 0.95,\ \delta = 0.01,\ r_p = 0.1,\ l_0 = 3,\ d = 2$ and $z = 4$. In terms of axial diffusion, the value $m = 2$ corresponds to axially symmetric stenosis, whereas $m = 2.5,\ 3.0,\ 3.5$ and 3.8 exhibit the effects of asymmetric stenosis. The effective axial diffusion is substantially larger in the arteries with symmetric stenosis than in the arteries with asymmetric stenosis. The increase in the stenosis shape parameter m results in decreasing viscosity which is in line with Biswas and Chakraborty [54] findings. Therefore, the blood moves slower along the axial distance. Since the increase of viscosity tends to reduce velocity, the effective diffusion is reduced. The radius of the stenosed artery $R(z)$ decreases from $R(z) = 0.973,\ 0.972,\ 0.827,\ 0.618$ to 0.340 with the increase of stenosis shape parameter m. As there are only minor changes as time passes, it is concluded that the effective axial diffusion is independent of time t.

Figure 6 (a) illustrates the variation of effective axial diffusion over time t for various plug core radius r_p when $\beta = 0.1,\ t = 0.1,\ n = 0.95,\ R(z) = 0.827,\ \delta = 0.01, l_0 = 3,\ d = 2,\ z = 4$ and $m = 3$. The effective axial diffusion is found to decrease slightly as the plug core radius increases. This is due to the high concentration of blood that accumulated at the centre, which reduces the solute transport. The effective axial diffusion is almost time-independent and is determined solely by the values of r_p. The effective axial diffusion increases slowly in the beginning until $t = 0.1$, after which it almost becomes constant. The constant values imply

that the effective axial diffusion reaches a steady-state, indicating that the drug is effective when the rate of drug intake equals the rate of drug elimination. The steady-state values are useful to determine the time needed to reach the steady-state dispersion and the reduction in solute dispersion caused by yield stress.

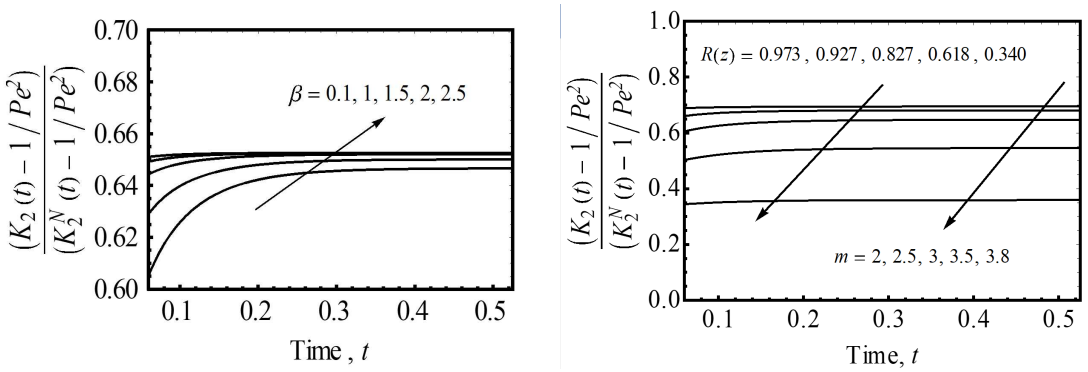

(a) (b)

Figure 5: Variation of effective axial diffusion over time t when $t = 0.1,\ n = 0.95, r_p = 0.1,\ \delta = 0.01,\ l_0 = 3,\ d = 2$ and $z = 4$ for (a) various chemical reaction rate parameter β (b) various stenosis shape parameter m

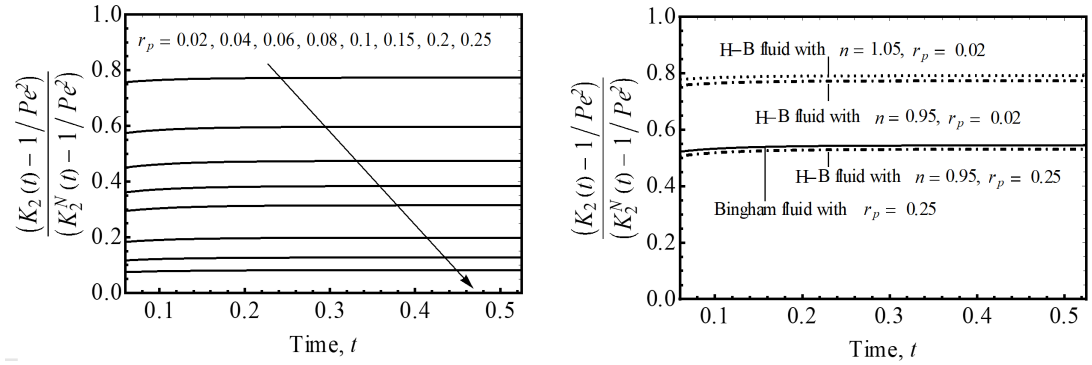

(a) (b)

Figure 6: Variation of the effective axial diffusion over time t when $\beta = 0.1,\ t, 0.1,\ R(z) = 0.827,\ \delta = 0.01, l_0 = 3,\ d = 2,\ z = 4$ and $m = 3$ for (a) various plug core radius r_p (b) various fluids

Figure 6 (b) shows the effective axial diffusion over time t for various fluids when $\beta = 0.1,\ t = 0.1,\ R(z) = 0.827,\ \delta = 0.01, l_0 = 3,\ d = 2,\ z = 4$ and $m = 3$. The solute disperses more rapidly in the Bingham fluid ($n = 1$) than in the H-B fluid ($n = 0.95$). As the power-law index increases, the effective axial diffusion also increases. The power-law index is dependent on the blood constituents, such as haematocrit, fibrinogen and cholesterol. The fluid exhibits shear-thinning behaviour when $n = 0.95$, shear-thickening behaviour when $n = 1.05$ and linear behaviour when $n = 1$ [55]. As mentioned by Hussain et al. [56], the power-law index displays the apparent whole blood viscosity. When the power-law index decreases, so does the viscosity. The solute disperses faster in the Bigham fluid than in the H-B fluid since the former has a higher viscosity than the latter. Based on the results, the H-B fluid exhibits a more realistic model for explaining the blood rheology in narrow arteries.

4 Conclusion

In summary, the issue of unsteady solute dispersion in blood flow by incorporating a first-order chemical reaction in the bulk flow via an asymmetry stenosed artery using GDM is solved by varying the physical parameters. The blood is presumed to be a non-Newtonian fluid (H-B fluid model) and flows in a rigid arterial wall. The yield stress plays an essential role in the determination of blood viscosity and velocity profiles in the blood flow. The solute dispersion coefficient and solute effective axial diffusion decrease with an increase in the yield stress of the blood flow. The solute dispersion coefficient descends with the raise of the chemical reaction parameter, stenosis shape parameter and power-law index. As these parameters increase, the concentration of red blood cells at the centre of the vessels also increases due to the degree of the solute binding to blood proteins. The solute effective axial diffusion increases with an increase of the chemical reaction parameter and power-law index. Conversely, as the stenosis shape parameter increased, the effective axial diffusion decreased. From the mathematical analysis, it was found that there is a substantial difference between the flow quantities computed with and without a chemical reaction and stenosis. Hence, this study contributes to the development of mathematical modelling as the H-B fluid model realistically demonstrated the blood rheology of the reactive dispersion in the blood flow through a narrow stenosed arteries. Considering blood flow is naturally throbbing, further research on the effects of pulsatile flow on fluid dispersion with the effect of chemical reactions would be beneficial.

Acknowledgments

The authors would like to acknowledge Research Management Centre, Universiti Teknologi Malaysia (UTM) for the financial support through GUP Tier 2 (Vote number Q.J130000.2654.17J12), and also Ministry of Higher Education (MOHE) under the research grant Fundamental Research Grant Scheme (FRGS/1/2020/STG06/UTM/02/15), (FRGS/1/2019/STG06/UTM/02/21) and UTM Fundamental Research (PY/2019/01623-Q.J130000.2554.21H48).

Nomenclature

Greek Symbols

$\bar{\beta}$	Chemical Reaction Parameter
β	Non-Dimensional Chemical Reaction Parameter
$\bar{\delta}$	Stenosis Height $[m]$
δ	Non-Dimensional Stenosis Height
$\bar{\tau}$	Shear Stress $[\mathrm{N}/m^2]$
τ	Non-Dimensional Shear Stress
$\bar{\tau}_y$	Yield Stress $[\mathrm{N}/m^2]$
τ_y	Non-Dimensional Yield Stress
η_H	H-B Fluid Viscosity Coefficient with Dimension $(ML^{-1}T^{-2})^n\, T[\mathrm{Ns}/m^2]$
λ_m	Roots of Equation $J_1\,(r) = 0$
ψ	Azimuthal Angle

Upper alphabetical letters

$\bar{A}$	Amplitude Parameter
A	Non-Dimensional Amplitude Parameter
$\bar{C}_0$	Reference Concentration
$\bar{C}$	Solute Concentration
C	Non-Dimensional Solute Concentration
C_m	Non-Dimensional Mean Concentration
D_m	Coefficient of Mass Diffusion
J_0	Bessel's Functions of The First Kind of Order Zero
J_1	Bessel's Functions of The First Kind of Order One
K_1	Longitudinal Convection Coefficient
K_2	Longitudinal Dispersion Coefficient
K_2^N	Newtonian Fluid Dispersion Coefficient
$\bar{L}$	Artery Length $[m]$
L	Non-Dimensional Artery Length
Pe	Modified Peclet Number
$\bar{R}(\bar{z})$	Radius of Stenosed Artery $[m]$
$R(z)$	Non-Dimensional Radius of Stenosed Artery
R_0	Arterial Radius

Lower alphabetical letters

$\bar{d}$	Stenosis Location $[m]$
d	Non-Dimensional Stenosis Location
f_{1s}	Dispersion Function in Steady-State
f_{1s_-}	Steady Dispersion Function in Plug Flow Field
f_{1s_+}	Steady Dispersion Function in Outer Flow Field
f_{1t}	Dispersion Function in Transient-State
f_1	Dispersion Function
$\bar{l}_0$	Length of Stenosis $[m]$
l_0	Non-Dimensional Length of Stenosis
m	Stenosis Shape Parameter
n	Power-law Index
$\bar{p}$	Pressure $[Pa]$
p	Non-Dimensional Pressure
$\bar{r}$	Transverse (Radial) Distance $[m]$
r	Non-Dimensional Transverse (Radial) Distance
$\bar{r}_p$	Plug Flow Radius $[m]$
r_p	Non-Dimensional Plug Flow Radius
$\bar{t}$	Time $[s]$
t	Non-Dimensional Time
$\bar{u}$	Velocity of Fluid $[m/s]$
u	Non-Dimensional Velocity of Fluid
u_0	Centreline Velocity $[m/s]$
u_-	Non-Dimensional Velocity in Plug Flow Field
u_+	Non-Dimensional Velocity in Non- Plug Flow Field

u_m Non-Dimensional Mean Velocity
$\bar{z}$ Longitudinal (Axial) Distance $[m]$
z Non-Dimensional Longitudinal (Axial) Distance

References

[1] Taylor, G. I. Dispersion of soluble matter in solvent flowing slowly through a tube. *Proceedings of the Royal Society of London. Series A. Mathematical and Physical Sciences*. 1953. 219(2): 186-203.

[2] Aris, R. On the dispersion of a solute in a fluid flowing through a tube. *Proceedings of the Royal Society of London. Series A. Mathematical and Physical Sciences*. 1956. 235(4): 67-77.

[3] Gill, W. and Sankarasubramanian, R. Exact analysis of unsteady convective diffusion. *Proceedings of the Royal Society of London. Series A. Mathematical and Physical Sciences*. 1970. 316(1): 341-350.

[4] Rana, J. and Murthy, P. Unsteady solute dispersion in Herschel-Bulkley fluid in a tube with wall absorption. *Physics of Fluids*. 2016. 28(11): 1119-1125.

[5] Jaafar, N. A., Yatim, Y. M. and Sankar, D. Mathematical analysis for unsteady dispersion of solute with chemical reaction in blood flow. In *AIP Conference Proceedings*. AIP Publishing LLC. 2016. 331–337.

[6] Sankar, D., Jaafar, N. A. and Yatim, Y. M. Mathematical analysis for unsteady dispersion of solutes in blood stream—A comparative study. *Journal Global Journal of Pure Applied Mathematics*. 2016. 12(2): 1337-1374.

[7] Balachandra, H., Rajashekhar, C., Vaidya, H., Oudina, F. M., Manjunatha, G. and Prasad, K. V. Homogeneous And Heterogeneous Reactions on The Peristalsis of Bingham Fluid with Variable Fluid Properties Through a Porous Channel. *Journal of Advanced Research in Fluid Mechanics Thermal Sciences.* 2021. 88(3): 1-19.

[8] Kori, J. Effect of first order chemical reactions on the dispersion coefficient associated with laminar flow through fibrosis affected lung. *Journal of Biomechanics*. 2020. 99(1): 109494.

[9] Roy, A. K., Saha, A. K., Ponalagusamy, R. and Debnath, S. Mathematical model on magneto-hydrodynamic dispersion in a porous medium under the influence of bulk chemical reaction. *Korea-Australia Rheology Journal.* 2020. 32(4): 287-299.

[10] Rana, J. and Murthy, P. Solute dispersion in pulsatile Casson fluid flow in a tube with wall absorption. *Journal of Fluid Mechanics.* 2016. 793(14): 877-914.

[11] Debnath, S., Saha, A., Mazumder, B. and Roy, A. Dispersion of reactive species in Casson fluid flow. *Indian Journal of Pure Applied Mathematics.* 2020. 51(4): 1451-1469.

[12] Roy, A., Saha, A. and Debnath, S. Effect of multiple reactions on the transport coefficients in pulsatile flow through an annulus. *International Communications in Heat Mass Transfer.* 2020. 110(4): 104369.

[13] Das, D., Poddar, N., Dhar, S., Kairi, R. R. and Mondal, K. K. Multi-scale approach to analyze the dispersion of solute under the influence of homogeneous and inhomogeneous reactions through a channel. *International Communications in Heat Mass Transfer. 2021.* 129(6): 105709.

[14] Orizaga, S., Riahi, D. N. and Soto J. R. Drug delivery in catheterized arterial blood flow with atherosclerosis. *Journal Results in Applied Mathematics*. 2020. 27(7): 100117.

[15] Roy, A.K. and Bég, O.A. Asymptotic study of unsteady mass transfer through a rigid artery with multiple irregular stenoses. *Applied Mathematics Computation*. 2021. 410(2): 126485.

[16] Carvalho, V., Pinho, D., Lima, R. A., Teixeira, J. C. and Teixeira, S. Blood flow modeling in coronary arteries: A review. *Fluids.* 2021. 6(2): 53.

[17] Ali, N., Zaman, A., Sajid, M., Nieto, J. and Torres, A. Unsteady non-Newtonian blood flow through a tapered overlapping stenosed catheterized vessel. *Mathematical Biosciences.* 2015. 269(15): 94-103.

[18] Abbas, Z., Shabbir, M. and Ali N. Analysis of rheological properties of Herschel-Bulkley fluid for pulsating flow of blood in stenosed artery. *AIP Advances*. 2017. **7**(10): 105123.

[19] Shah, S. R. Study of modified Casson's fluid model in modeled normal and stenotic capillary-tissue diffusion phenomena. *International Journal of Computational Engineering and Management*. 2011. 11(2): 51-57.

[20] Mishra, S. and Siddiqui, S. A mathematical model for flow and diffusion through stenotic capillary-tissue exchange system. *Electronic Journal Science and Technology*. 2015. 17(4): 299-315.

[21] Sriyab, S. Mathematical analysis of non-Newtonian blood flow in stenosis narrow arteries. *Computational and Mathematical Methods in Medicine*. 2014. 2014(2): 1-10.

[22] Sankar, D. and Hemalatha, K. Pulsatile flow of Herschel–Bulkley fluid through stenosed arteries—a mathematical model. *International Journal of Non-Linear Mechanics*. 2006. 41(8): 979-990.

[23] Hossain, K. E. and Haque, M. M. Influence of magnetic field on chemically reactive blood flow through stenosed bifurcated arteries. In AIP Conference Proceedings. 2017. 1-12.

[24] Freidoonimehr, N., Chin, R., Zander, A. and Arjomandi, M. An experimental model for pressure drop evaluation in a stenosed coronary artery. *Physics of Fluids*. 2020. 32(4): 021901.

[25] Prashantha, B. and Anish, S. Discrete-Phase modelling of an asymmetric stenosis artery under different womersley numbers. *Arabian Journal for Science and Engineering.* 2019. 44(6): 1001-1015.

[26] Alsemiry, R. D., Mandal, P. K., Sayed, H. M. and Amin, N. Numerical solution of blood flow and mass transport in an elastic tube with multiple stenoses. BioMed Research International 2020. 2020(12): 1-14.

[27] Bakheet, A. and Alnussairy, E. A. Numerical Simulation of Magnetohydrodynamic Influences on Casson Model for Blood Flow through an Overlapping Stenosed Artery. Iraqi Journal of Science. 2021. 62(4): 1016-1024.

[28] Majee, S. and Shit, G. Modeling and simulation of blood flow with magnetic nanoparticles as carrier for targeted drug delivery in the stenosed artery. *European Journal of Mechanics-B/Fluids*. 2020. 83(4): 42-57.

[29] Tiwari, A., Shah, P. D. and Chauhan S. S. Unsteady solute dispersion in two-fluid flowing through narrow tubes: A temperature-dependent viscosity approach. *International Journal of Thermal Sciences.* 2021. 161(4): 106651.

[30] Rana, J. and Liao, S. A general analytical approach to study solute dispersion in non-Newtonian fluid flow. *European Journal of Mechanics-B/Fluids.* 2019. **77**(3): 183-200.

[31] Ratchagar, N.P. and Vijayakumar, R. Dispersion of a solute in a couple stress fluid with chemical reaction using generalized dispersion model. *Advances in Mathematics: Scientific Journal.* 2020. 4(9): 2233-2247.

[32] Rana, J. and Murthy, P. Unsteady solute dispersion in small blood vessels using a two-phase Casson model. *Journal Proceedings of the Royal Society A: Mathematical, Physical Engineering Sciences.* 2017. 473(2204): 201-217.

[33] Sebastian, B. and Nagarani P. On convection-diffusion in non-Newtonian fluid flow in an annulus with wall oscillations. *The European Physical Journal Special Topics.* 2019. 228(12): 2729-2752.

[34] Dash, R., Jayaraman, G. and Mehta K. Shear augmented dispersion of a solute in a Casson fluid flowing in a conduit. *Annals of Biomedical Engineering.* 2000. 28(4): 373-385.

[35] Ramana, B., Sarojamma, G., Vishali, B. and Nagarani, P. Dispersion of a solute in a Herschel-Bulkley fluid flowing in a conduit. *Journal of Experimental Sciences.* 2012. 3(2): 14-23.

[36] Blair, G. and Scott, W. *An introduction to biorheology.* New York: Elsevier. 1974.

[37] Chaturani, P. and Ponnalagarsamy, R. A study of non-Newtonian aspects of blood flow through stenosed arteries and its applications in arterial diseases. *Biorheology.* 1985. 22(6): 521-531.

[38] Tu, C. and Deville M. Pulsatile flow of non-Newtonian fluids through arterial stenoses. *Journal of biomechanics.* 1996. 29(7): 899-908.

[39] Amalraj, I. J., Narasimman, S. and Kandasamy, A. Rheodynamic lubrication of an externally pressured thrust bearing using herschel-bulkley fluid with sinusoidal injection. *Journal of applied fluid mechanics.* 2012. 5(4): 71-79.

[40] Ponalagusamy, R. and Priyadharshini, S. A numerical model on pulsatile flow of magnetic nanoparticles as drug carrier suspended in Herschel–Bulkley fluid through an arterial stenosis under external magnetic field and body force. *International Journal of Computer Mathematics.* 2019. 96(9): 1763-1786.

[41] Hamed, S.B. and Belhadri, M. Rheological properties of biopolymers drilling fluids. *Journal of Petroleum Science Engineering.* 2009. 67(3-4): 84-90.

[42] Kanin, E., Dontsov, E., Garagash, D. and Osiptsov, A. A radial hydraulic fracture driven by a Herschel–Bulkley fluid. Journal of Non-Newtonian Fluid Mechanics. 2021. 295: 104620. Coelho, P. M. and Poole, R. J. Heat transfer in laminar flow of a Herschel-Bulkley fluid between parallel plates. *Heat Transfer Engineering.* 2021. 45(2): 1-22.

[43] Coelho, P. M. and Poole, R. J. Heat transfer in laminar flow of a Herschel-Bulkley fluid between parallel plates. Heat Transfer Engineering. 2021. 45(2): 1-22.

[44] El-dabe, N. T., Abou-zeid, M. Y., Mohamed, M. A. and Maged, M. Peristaltic flow of Herschel Bulkley nanofluid through a non-Darcy porous medium with heat transfer under slip condition. *International Journal of Applied Electromagnetics Mechanics.* 2021. 45(2): 1-19.

[45] Swarup, S. *Fluid Dynamics*. Uttar Pradesh: Elsevier. 2000.

[46] Debnath, S. and Ghoshal, K. Transport of reactive species in oscillatory Couette-Poiseuille flows subject to homogeneous and heterogeneous reactions. *Applied Mathematics and Computation*. 2020. 385: 125387.

[47] Sankar, D. and Lee, U. Mathematical modeling of pulsatile flow of non-Newtonian fluid in stenosed arteries. *Communications in Nonlininear Science and Numerical Simulation*. 2009. 14: 2971-2981.

[48] Singh, A., Shrivastav, R. and Bhatnagar, A. A numerical analysis for the effect of slip velocity and stenosis shape on Non-Newtonian flow of blood. *International Journal of Engineering*. 2015. 28: 440-446.

[49] Misra, J. and Shit, G. Blood flow through arteries in a pathological state: A theoretical study. *International Journal of Engineering Science.* 2006. 44: 662-671.

[50] Shukla, J., Parihar, R. and Rao, B. Dispersion in non-Newtonian fluids: Effects of chemical reaction. *Rheologica Acta*. 1979. 18: 740-748.

[51] Singh, S., Chadda, G. and Sinha, A. A study of sectionally related dispersion and chemical reaction effects. Defence Science Journal. 1989. 39: 305.

[52] Sankar, D. and Nagar, A. K. Nonlinear fluid models for biofluid flow in constricted blood vessels under body accelerations: A comparative study. *Journal of Applied Mathematics*. 2012. 2012(4): 1-27.

[53] Jaafar, N. A. *Mathematical Analysis of Herschel-Bulkley Fluid Model for Solute Dispersion in Blood Flow through Narrow Conduits*. Ph.D. Thesis. Universiti Sains Malaysia. 2017.

[54] Biswas, D., and Chakraborty, U. S. Pulsatile blood flow through a catheterized artery with an axially nonsymmetrical stenosis. *Applied Mathematical Sciences.* 2010. 58: 2865-2880

[55] Misra, J.C., Shit, G.C. and Pramanik, R. Non-Newtonian flow of blood in a catheterized bifurcated stenosed artery. *Journal of Bionic Engineering*. 2018. 15: 173-184.

[56] Hussain, M. A., Kar, S. and Puniyani, R. R. Relationship between power law coefficients and major blood constituents affecting the whole blood viscosity. *Journal of Biosciences*. 1999. 24: 329-337.